Office of Naval Research

Contract Nonr-401(44)

Task No. NR 051-428

Technical Report No. 4

by

Peter Sullivan

and

Bernhard Wunderlich

To be submitted as part of a
M.S. Thesis to the Graduate School of
Cornell University

(A shortened version will be submitted to the SPE Transactions for possible publication).

Cornell University
Department of Chemistry
Ithaca, N.Y.
May 30, 1963

INTERFERENCE MICROSCOPY
OF
HIGH POLYMERS

PREFACE

The research conducted under the Contract Nonr 401 (44) is entitled: "Polymers at High Pressure". Interference Microscopy has been developed in this connection as a service tool to analyze the morphology of polymer samples crystallized at elevated pressure. The results obtained were so satisfactory, however, that it was also undertaken to use this tool for studies of morphology of atmospheric pressure crystallized polymers and an investigation of the thermodynamics of melting of polymer single crystal lamellae.

In this thesis, P. Sullivan describes the different kinds of interference microscopy as applied to polymer research in this laboratory. The principle polymer used is a linear polyethylene.

P. Sullivan received additional financial help for the different phases of research from the Advanced Research Projects Agency (1960/62) and the National Science Foundation (1962/63). This support is gratefully acknowledged.

Bernhard Wunderlich
Project Director

I. INTRODUCTION

Linear or normal paraffins are easily crystallized from solution. Both slow and fast cooling of such solutions usually give platy crystals. In a similar fashion, some linear high polymers can be crystallized from slowly cooled solutions. The discovery of this phenomenon, though, has been relatively recent.[1,2,3]

The polymer crystals grown from solution are usually extremely small, and so must be observed with an electron microscope. The optical microscope can be used when somewhat larger crystals are grown. The high magnification of the electron microscope limits the area viewed, so that only a few crystals can be observed. Furthermore, the electron beam in this type of microscopy destroys the crystal after a short time, so that it becomes useless for continued examination (as for example by electron diffraction[4]). Typical precision in the measurement of platelet thickness by means of the electron microscope[5] is $\pm$10Å.

It is quite difficult to observe paraffin or polyethylene single crystals with an ordinary optical microscope, since the contrast of the crystals is small. However, the use of interference microscopes of various types or the proper preparation of the crystals enables one to easily observe the platelets. As opposed to the electron microscope, a far larger field of view can be observed and the

crystals are left intact by these methods. The precision in thickness measurement can exceed that of the electron microscope and low angle X-ray methods.

Optical interferometry has been extensively developed for the investigation of crystal properties[6,7]. Tolansky has developed the techniques of multiple beam interferometry so that distances as small as three Angstrom units in depth can be resolved.[6] These methods of investigation are particularly well suited for the measurement of the thicknesses of normal paraffins and normal carboxylic acids. For the latter two cases, the thicknesses of monomolecular platelets are estimated from the number of carbon atoms in the molecule and the carbon-carbon bond distance (and the carbon-oxygen bond distance for the acids). That the platelets can indeed be monomolecular has been shown by several workers. For example, Dawson and Vand have measured the thicknesses of single crystals of $C_{36}H_{74}$ (n-hexatriacontane) and $C_{39}H_{80}$ (n-nonatriacontane) as 43 ± 5 Å and 45 ± 10 Å respectively.[5,8] Courtney-Pratt has measured the thicknesses of monomolecular films of $C_{17}H_{35}COOH$ (stearic acid) and $C_{27}H_{55}COOH$ (octacosanoic acid) by multiple beam interferometry. The thicknesses were 19 ± 3 Å and 30 ± 1 Å respectively.[9] The thicknesses of polyethylene single crystals have been found to vary from about 100 Å up to 400 Å (the latter value having been obtained for annealed single crystals).[10,11]

One might also mention the method of low-angle X-ray diffraction as a means of measurement of the thickness of crystals of the order of 100 Å. This method necessitates the use of a large number of crystals and so one can only measure the average thickness. The methods of electron microscopy and interference microscopy both allow one to perform measurements on an individual crystal and so are somewhat superior to that of low-angle X-ray diffraction.

In this thesis, several methods of interference microscopy will be discussed, as well as the utilization of these methods in the determination of the heights of single crystals of a linear polyethylene. Growth spirals, which may develop from the platelets, will also be considered. Spherulitic and dendritic structures will be treated only qualitatively in a description of the morphology of the solution crystallization of linear polyethylene. The methods discussed are two beam interference microscopy (the Baker interference microscopy[12] and the two beam interferometer developed by Nomarski[13]), Newton's rings, and multiple beam interferometry.

II. INTERFERENCE MICROSCOPY

There are a large number of interferometers available, some of which, can be adapted to the microscope. These are discussed in suitable texts[7,14]. For example, one could mention the method of phase contrast microscopy, which has been used for the qualitative observation of polymer solution grown crystals[15,16]. The methods of two beam interference microscopy described in the following pages were chosen because of their adaptation to the experiments of interest.

The refractive indices of polyethylene crystals are between 1.5 and 1.6 (see later) for the λ = 5461Å line of mercury. If one divides a ray of light into two separate coherent rays and later causes them to recombine, they can interfere if the optical paths of the two rays are different. For example, one of the coherent beams could pass through a polyethylene single crystal and the other through a mounting medium of a different refractive index. On recombination, the two rays can interfere because of the optical path differences. In this fashion, the difference in phase of the two rays is converted into an intensity difference and thus makes the crystal visible. This method is particularly useful for the observation of crystals which show little contrast otherwise.

a_1) Two beam interference microscopy. The Baker interference microscope[12].

Division of a ray of light as described above is a common phenomena through the use of doubly refractive crystals. If a light ray is incident onto a uniaxial crystal (i.e., a crystal with two principal indices of refraction) at some angle with the optic axis, in general two rays will result: the ordinary ray, whose vibration direction is perpendicular to the plane of the optic axis and ordinary ray, and the extraordinary ray, whose vibrational direction is in the plane of the optic axis and the extraordinary ray.[i,17] Such a division of a light ray is the basis of the Baker interference microscope, which is the first method of two beam interference microscopy described.[10,18]

The essential optical elements of this microscope are the polarizer, condenser, double refraction plates, objective, quarter wave plate, analyzer, and the eyepiece. A schematic diagram of the arrangement of these components is given in Fig. 1 and the function of each is described in the following paragraphs.

Starting from the bottom of the diagram, the polarizer causes the incident monochromatic light to vibrate in a single plane.[ii] The condenser collects this linearly

i) The vibration direction is taken as that of the electric vector. In isotropic media, this is perpendicular to the propagation direction of the light ray.

ii) If the vibration direction of the electric vector lies in a single plane for one complete period of the ray, the light will be called linearly polarized.

polarized light, which then passes through the first doubly refractive plate, and focuses it on the specimen.

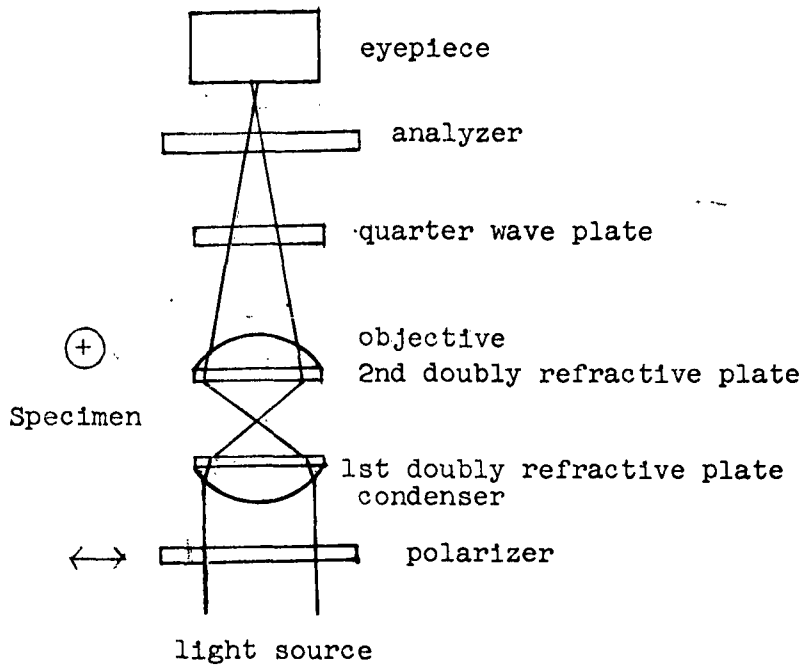

Figure 1

The optic axis of the first doubly refractive plate is in the plane of the paper as indicated by the double headed arrow of Fig. 1. The plane of vibration of the polarizer is at an angle of 45° out of the plane of the paper, so that ideally (i.e., no rotation of the vibration direction of the non-axial rays by the condenser; this actually does occur and is discussed by Kamb[19]) two rays of equal intensity but linearly polarized at right angles to each other emerge

from the first doubly refractive plate for each ray entering. These two rays can both pass through the sample, both bypass the sample or one pass through and the other pass beside the sample. It is the last instance which leads to contrast between the specimen and the mounting medium, so that the specimen becomes visible.

The condenser focuses the light from the illuminator onto the specimen. Accordingly, rays which enter the specimen at different angles will travel different distances inside the sample. This is shown schematically in Fig. 2.

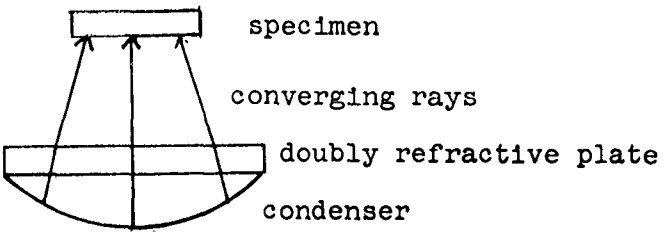

Figure 2

The optical path difference between the ray passing through the sample and that passing beside is:

(1) $\Delta_1 = (n_1 - n_2)t$, where n_1 = refractive index of the sample

n_2 = refractive index of the mounting medium

t = thickness of the sample

Note in particular that the index n_1 is not necessarily a principal refractive index of the crystal specimen. As was just pointed out above, the rays emerging from the condenser are converging onto the specimen, and so the value of n_1 depends on the angle at which the rays enter the crystal and on the orientation of the principal refractive indices in the crystal. The thickness, t, will be an average value over the distances the rays travel inside the crystal sample.

The rays leaving the crystal specimen now enter the second doubly refractive plate and then the objective. In order to recombine the two coherent rays, the optic axis of the second plate may be parallel to that of the first plate, in which case a half-wave plate must be introduced between the two plates. Alternatively, the optic axis of the second plate may be perpendicular to that of the first plate (and to the plane of the paper), so that no half-wave plate is necessary. Both arrangements allow the ordinary ray of the first plate to become the extraordinary ray of the second plate; also, the extraordinary ray of the first plate becomes the ordinary ray of the second plate. The only path difference between the two rays as they enter the objective is caused by the specimen.

Figure 3 is a diagram of the doubly refractive plates. The arrow in I indicates the orientation of its optic axis

and similarly, the cross in II indicates the orientation

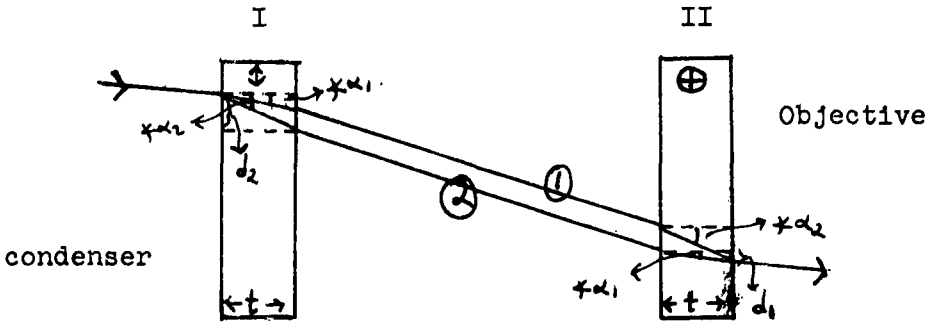

Figure 3

of its optic axis which is rotated 90 degrees. The lateral separation of the two rays leaving I is $d_2 - d_1$, where $d_2 = t(\tan \alpha_2)$ and $d_1 = t(\tan \alpha_1)$. Since the optic axis of II has been rotated 90° relative to that of I, ray 1 will be refracted through angle α_2 and ray 2 through angle α_1 (in II). This allows the two laterally separated rays to recombine into a single linearly polarized ray, as was initially incident onto I.

If an isotropic substance is now placed in the path of ray 1, this ray will be displaced (due to refraction). This displacement will be small as long as the substance is very thin so that rays 1 and 2 can combine into one ray in II which is elliptically polarized. The path difference between the components of this elliptically polarized ray is only due to the substance and is given by equation (1).

Instead on an isotropic substance, suppose the object placed in the path of ray 1 is anisotropic. More specifically, let this object be a uniaxial crystal (two principal indices of refraction). In general, ray 1 will be refracted by this crystal, giving rise to ordinary and extraordinary rays in the crystal. Assuming that the crystal thickness is of the order of 100Å and that the indices of the ordinary and extraordinary rays are not widely different, then these two rays will approximately travel along the same direction. There will be an optical path difference between the two rays, given by:

(2) $\Delta_2 = (n_o - n_e)t$, where n_o = ordinary index of the anisotropic crystal,

n_e = extraordinary index of the anisotropic crystal, and

t = optical path,

so that the resulting rays emerging from the crystal specimen will appear as one elliptically polarized ray.

For the case of polyethylene single crystals, light is traveling through the crystal along paths close to the c-crystallographic axis, i.e., along paths close to the optic axis (assuming the crystal system is uniaxial; actually, there are two indices perpendicular to the optic axis, but these differ only by approximately 0.005, so

that polyethylene appears to be uniaxial instead of biaxial. This will be discussed later). Since t is small and n_e is close to n_o, Δ_2 is small. The path difference between ray 2 and ray 1 which has passed through a polyethylene single crystal (Fig. 3) when the two rays have been recombined by plate II is then approximately:

(3) $\Delta_2 = (\bar{n}_1 - n_2)t$ where $\bar{n}_1$ is the appropriate average refractive index.

The ray emerging from the second doubly refractive plate is accordingly assumed to be elliptically polarized for both cases, the isotropic and the anisotropic thin samples. Its analysis by the quarter wave plate and analyzer (Fig. 1) requires some discussion of elliptically polarized light.

Two linearly polarized rays traveling along the same path, vibrating in mutually perpendicular directions and having some difference in phase δ constitute what has been referred to as elliptically polarized light. Let the vibrations be along the x and y directions, and the rays travel or propagate along the z direction, perpendicular to the plane of the paper (Fig. 4). At a fixed position, the amplitude oscillation along the x direction follows the relation:

$$x_1 = a_1 \sin wt,$$

where a_1 is the maximum amplitude along the x-axis. Similarly, the amplitude variation along the y direction follows

the relation:

$$y_1 = b_1 \sin(wt + \delta),$$

where b_1 is the maximum amplitude along the y-axis and

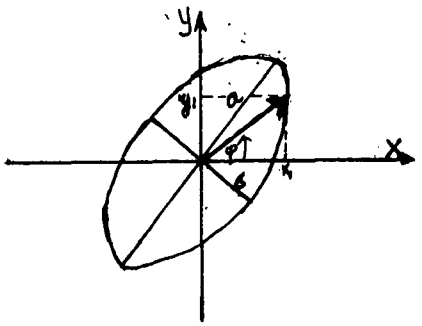

Figure 4

δ is the difference in phase between the two rays (t is the time and $w = 2\pi\nu$, where ν is the frequency of the ray). At this same fixed position and at some time t, the angle which the resultant (linearly polarized) ray makes with the x-axis can be computed from the relation:

$$(4) \qquad \tan \phi = \frac{y_1}{x_1} = \frac{b_1 \sin(wt + \delta)}{a_1 \sin wt} \quad ,$$

where ϕ is indicated in Fig. 4.

Physically, the same situation can be realized with two linearly polarized rays, vibrating in mutually perpendicular directions and traveling along the same path with difference in phase of $\frac{\pi}{2}$ if the amplitudes of the component rays are the semi-major and semi-minor axes of

the ellipse of Fig. 4. To analyze this elliptically polarized light, the quarter-wave plate is placed in the path of the ray with its optic axis parallel to either axis a or b of the diagram (Fig. 4). Since a quarter-wave plate introduces a phase difference of $\frac{\pi}{2}$, the emerging light ray will be linearly polarized. The angle which the plane of vibration of this linearly polarized ray makes with the a or b axis depends on the amplitudes a and b. One can transform the ellipse of Fig. 4 from the x,y coordinates to coordinates along a,b. This enables one to establish a relation between the plane of vibration of the now linearly polarized ray to the difference in phase δ.[14] The angle between the vibration direction of the resulting linearly polarized ray and the b coordinate (see Fig. 4) is α.

$$\tan \alpha = \frac{a}{b} .$$

α can be measured by means of the analyzer. The angle the vibration direction of the analyzer makes with the optic axis of the quarter wave plate at total extinction is α.

Once α has been determined, the difference in phase between the component rays of the elliptically polarized ray can be found. If $a_1 = b_1$, then it can be shown that[14]:

$$\sin 2\alpha = \sin \delta, \text{ or}$$

$$2\alpha = \delta = \frac{2\pi}{\lambda} (\Delta_3) = \frac{2\pi}{\lambda} (\Delta_1) \qquad (6)$$

Thus, one measures the extinction angle of the crystal specimen relative to the background, determining α. Knowing Δ_3 (or Δ_1) and using monochromatic light, one can then determine t, the thickness of the specimen.

The (American Optics) Baker interference microscope has the optic axis of the quarter wave plate fixed. Now, the orientation of the axes of the ellipse relative to the optic axis of the quarter-wave plate depends on the phase difference δ. Therefore one does not always obtain linearly polarized light emerging from the quarter-wave plate and in fact it must generally be elliptically polarized.

One still determines α, though, by comparing minima in intensity for background and crystal. If the quarter-wave plate were of proper orientation, one could obtain complete extinction. As it is, minima in intensity will be observed.

Both an ordinary and an extraordinary ray are generated in doubly refractive plate I (Fig. 3). Either one of these rays can pass through the specimen and they will each be retarded differently by the second doubly refractive plate (plate II). This gives rise to two images of the specimen. The microscope is constructed such that only one image can be focussed. The second image is separated laterally from the image in focus.

For the measurement of polyethylene single crystal thicknesses, several mounting media were tried, but air was found to give the maximum contrast with these crystals.[10] A half-shade eyepiece usually replaced the analyzer for the measurements on single crystals in order to achieve maximum precision. The illumination used was a low pressure mercury lamp, filtered so that the 5461Å line was isolated. Typical crystals grown from tetrachloroethylene are shown in Figs. 13--15.

The average value of α for the single platelet of Fig. 13 (indicated with an arrow) was found to be 2.2°. Substituting this value into equation 6, one finds that $t = 128Å$ ($\bar{n}_1 = 1.520$, $n_2 = 1.000$, $\lambda = 5461Å$).

Previous data on single crystals of polyethylene grown from toluene gave platelet thicknesses of $134 \pm 6Å$.[10] The precision of such data is better than that obtained with the electron microscope. Furthermore, as pointed out previously, the crystals are left intact by the optical methods, whereas the electron beam used in electron microscopy alters or destroys the original crystal.

a_2) Two beam interference microscopy. The Nomarski interferometer.[13]

The second method of two beam interference microscopy considered is based on the same principle as that of the Baker interference microscope, i.e., division of a ray of

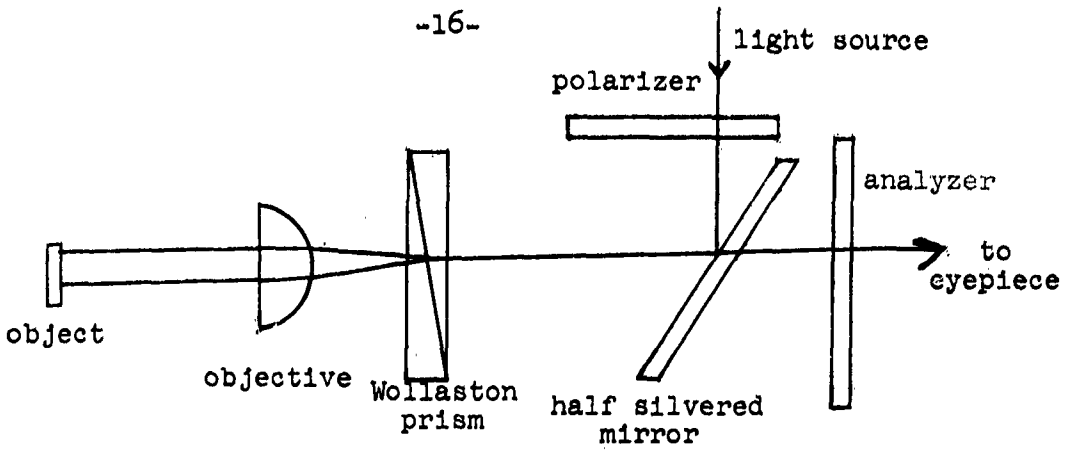

Figure 5

light by means of doubly refractive crystals. The particular type of doubly refractive crystal used is a quartz Wollaston prism, inserted into an ordinary incident light microscope. A schematic diagram of the components of the microscope used for the experiments described in this paper is given in Fig. 5.

The Wollaston prism is located at the focal plane of the objective, so that parallel light emerges from the objective onto the specimen. The prism itself is composed of two quartz prisms cemented together. The optic axes of the prisms are mutually perpendicular, as indicated by the arrow and cross in Fig. 6. The Wollaston prism in this particular arrangement is after Nomarski.[15]

An examination of the function of the Wollaston prism in the above arrangement will show how platelets or crystals with steps can be observed. A single ray of light with its vibration direction at an angle of 45° to

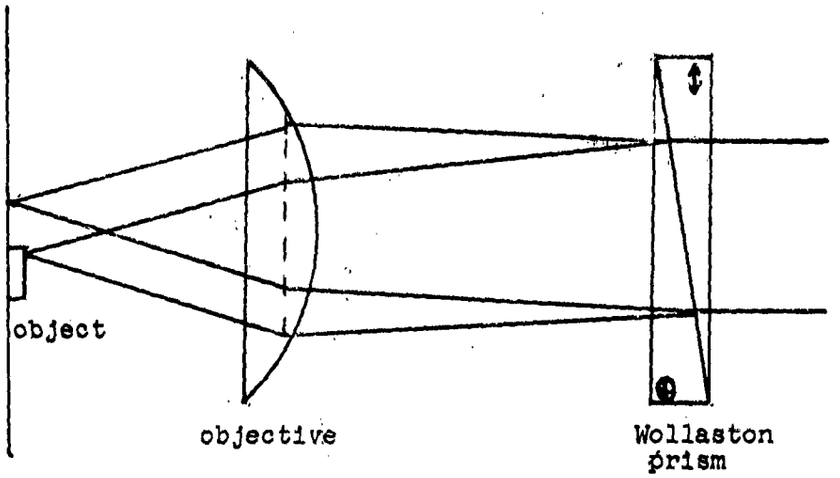

Figure 6

the vibration directions of the prism closest to the mirror (Fig. 5) is split into two rays upon reaching the second prism. These two rays diverge, and since the prism is located at the focal plane of the objective, emerge from the objective as parallel rays. The ray reflected from the object obviously travels a shorter path than its neighbor. For the ideal case shown, these two rays combine into a single elliptically polarized ray, the phase difference between the components of this ray being approximately $\frac{2\pi}{\lambda}(2t)$, where t is the thickness of the object. The analyzer is arranged so that its vibration direction is perpendicular to that of the polarizer. The entire field observed will then be dark (note: thin prisms are used), except where there are changes in height. These

elevations are the only cause of path differences in the rays emerging from the prism and so lead to bright regions on a dark field. In this way platelets and growth spirals are made visible (Figs. 12, 23). The refractive indices of the object affect the image formed only little, at least for the case of polyethylene. Figure 32 is a photomicrograph of a polyethylene growth spiral (which will be further described later) whose surface has been silvered (this process will also be described later). Most of the light incident onto such silvered crystals is reflected at the silver surface. Figure 12 is a micrograph of an unsilvered (and different) crystal. There are no significant differences in the images formed, so that one concludes that the light reflected at the bottom surfaces of the unsilvered crystals does not seriously interfere with the image formed by the top surface.

This microscope was found useful for the determination of single crystal melting points of polyethylene. A single growth spiral could easily be located and its liquifaction observed as the temperature was raised. The results of these melting experiments will be described later.

A second use was for the observation of crystals which had been silvered for observation by multiple beam methods. The silvered crystal, as pointed out above, reflects well. Thus, patterns observed as multiple beam interference fringes

could be correlated with the type of crystal viewed by means of the Nomarski interferometer.

b) Newton's rings method of interference microscopy.

This well known method of interferometry involves the use of a flat reflecting surface and a convex lens. The lens is brought into contact with the flat surface (Fig. 7) and the interference system formed observed with a microscope. For the case discussed here, the illumination is from above the lens and an incident light microscope is used.

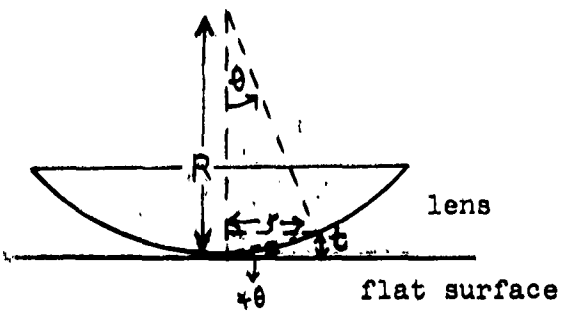

Figure 7

From Fig. 7, one has:

$$\tan \theta = \frac{t}{r} . \tag{7}$$

If θ is small, then approximately sin θ = tan θ, or

$$\frac{r}{R} = \frac{t}{r} \tag{8}$$

and so,

$$t = \frac{r^2}{R} . \tag{9}$$

Darkness occurs at the center where the two surfaces are in contact. The reason for this is that there is a difference in phase of π between the beam reflected at the bottom flat surface (air-glass) and the beam reflected at the curved lens surface (glass-air). These two beams must interfere destructively.

Darkness again occurs out from the central dark region wherever the distance between the two surfaces, t, is some multiple of $\frac{\lambda}{2}$, i.e., wherever:

(10) $$t = \frac{n\lambda}{2} \quad (n = 1,2,\ldots) \ .$$

Figure 22 is a photomicrograph of this interference system. The dark circles occur at the surface of the contact lens of Fig. 7 and are magnified by the microscope. The first few interference lines of Fig. 22 (starting from the center) are about 0.5 mm. in width. The first and second circles are separated by about 2.5 mm., so that a displacement of one fringe width would correspond to a height change of $\frac{0.5}{2.5}(\frac{\lambda}{2})$, which is approximately 600 Å for the illumination from a sodium lamp (λ = 5890Å).

Figure 23 is a micrograph of n-$C_{36}H_{74}$ crystals on a microscope slide (crystallized from n-propanol at 50.1°C, 2.1 mg. paraffin/g. solvent). Figure 24 is a micrograph of the same crystals after placing a convex contact lens (R = 3.0 mm.) in contact with the slide. Note that the

fringes are displaced slightly by the crystals. Since the edges of these crystals are relatively steep, one cannot count the number of fringes along the edges and so determine the integral number of $\frac{\lambda}{2}$ up to the actual fringe which is displaced in the micrograph.

Since polymer crystals are around 100 Å in thickness, this method could be applicable. At least one knows that most platelets are less than one-half wave length in thickness. The fringes of Fig. 22 are too thick to allow measurements of this order of magnitude and so increased accuracy was sought by silvering the surfaces, so that narrow fringes were obtained (the narrowing of the fringes by silvering will be discussed later). Figure 25 is a micrograph of the silvered system, which can be compared with Fig. 22 . No crystals are shown. Note that the center is bright. The reason for this is that phase changes of π occur at the lens-silver surface and also at the air-silver surface, so that the reflected beams are in phase at the center, giving a bright region.

An enlargement of Fig. 25 allowed more precise measurements to be performed on the figure. The line widths were found to be 0.5 mm., and the distance separating the two inner dark circles 20 mm. A displacement of one line width on these inner fringes would correspond to a height change of $\frac{0.5}{20}\left(\frac{\lambda}{2}\right)$, which is approximately 75Å for the light from

a sodium lamp. One sees that the silvering greatly increases the sensitivity of the method, and allows one to measure thicknesses of polymer platelets.

One difficulty found with this method was that the focusing of the fine interference lines for photographing is an extremely delicate process. A slight jarring of the microscope when the two silvered surfaces are in contact mars the silver and makes measurements in these regions impossible.

c) Multiple Beam Interferometry

In addition to the two beam methods of interferometry described above, there are available methods of greater resolution for the measurement of thickness. The use of multiple beams is one such method and, as mentioned previously, Tolansky has developed this technique so that distances as small as three Angstrom units in depth may be resolved.[6] Also, the techniques of measurement of wavelength differences as developed in spectroscopy can be applied to thickness measurements, as will be described shortly.

Polyethylene growth spirals appear pyramidal shaped under the optical and electron microscopes. The surfaces of these crystals are insufficiently reflecting to allow internal interference patterns to be observed, as Forty has done with cadmium iodide crystals.[20] However silvering both sides of the crystals allows the interference pattern

to become observable (under suitable illumination), as Verma has done with stearic acid.[21] The method to be described is of low or high resolution depending on the structure of the crystal.

The model used to explain the patterns seen in Figs. 16--19 is that of a pyramid with steps, as shown schematically in Fig. 8. If for the moment one consideres two parallel plates, then the condition for intensity maxima for the plates observed with transmitted light is:

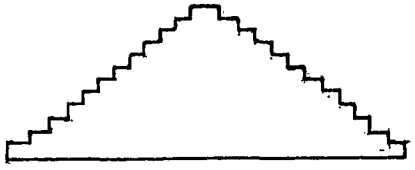

Figure 8

(11) $(2\mu t)\cos\phi = n\lambda$, $n=1,2,\ldots,$

μ=refractive index of region between plates

t=thickness between plates, and

ϕ=angle of refraction inside plate.

If the plates are illuminated with parallel light incident normally onto the first surface, then $\phi=0$, and one has:

(12) $2\mu t = n\lambda$

Returning to the pyramid of Fig. 8 above, if it is illuminated with parallel monochromatic light incident normally onto its bottom surface, then maxima in intensity

occur wherever:

$$t = \frac{n\lambda}{2\mu}, \quad n=1,2,\ldots$$

However, polyethylene crystals are so transparent that these maxima cannot be distinguished from the directly transmitted light. If one silvers the bottom and top surfaces of the crystal, then one in effect allows only a very small portion of the incident light to be transmitted by the crystal and the maxima are easily visible (Figs. 16--19).

The sharpening of the fringes can be interpreted in terms of the reflection coefficient, r, of the surface on which the light is incident (r is defined as the fraction of the incident light reflected by the surface). Consider two plane parallel plates with a single beam of light of amplitude E_o incident on the top surface, Fig. 9. If the fractions reflected internally and externally are the same (r), then the total intensity of the transmitted light can be shown to obey the relation:[17]

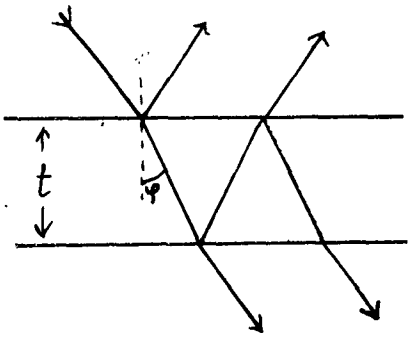

Figure 9

$$(13) \qquad I_t = \frac{I_o}{1 + \frac{4r^2}{(1-r^2)^2} \sin^2 \frac{\delta}{2}} ,$$

where

$$\delta = \frac{2\pi}{\lambda}(2\mu t)\cos\phi,$$

ϕ = angle of refraction in the medium.

δ is the difference in phase between two successive transmitted rays. Again, for $\phi=0°$,

$$\delta = \frac{2\pi}{\lambda}(2\mu t).$$

No absorbtion of the light is assumed to occur. For large r, i.e., close to one, I_t is an extremely sensitive function of δ. This function has its maxima at $\delta=m2\pi$, where m = 0,1,2,... Plots of I_t/I_o versus δ rapidly decrease near the maxima when r is near one. Figure 33 is a graph of I_t/I_o versus t. Curves for two values of r are plotted, one for r = 0.2 and the other for r = 0.9. The maxima occur, as expected, wherever $t=n\lambda/2\mu$.

A reflection coefficient of 0.9 was attained by evaporating a sufficient thickness of silver metal onto the polyethylene crystal surfaces. All the multiple beam interference photographs presented were taken with r at least 0.9. A value of r = 0.2 is approximately the reflection coefficient for polyethylene crystals when illuminated at normal incidence. This can be shown by the relation (Fresnel):[17]

(14) $$r = \frac{n-1}{n+1} = \frac{1.5-1}{1.5+1} = \frac{0.5}{2.5} = 0.2.$$

A glance at the graph (Fig. 33) shows that the intensity minima are around 0.85 of the maxima, when r = 0.2. One would expect from this consideration that the maxima would hardly be distinguishable from the minima, as is found when the crystals are unsilvered.

For $t = \frac{5.4\lambda}{12\mu} = .1620$Å ($\lambda = 5461$Å, $\mu = 1.52$), the intensity ratio has practically reached its minimum value $\frac{I_t}{I_o} = 0.116$ ($r = 0.9$). Passing over the intensity maxima the intensity ratio again reaches 0.116 at $t = \frac{6.6\lambda}{12\mu}$. The change in thickness is $\Delta t = \frac{1.2\lambda}{12\mu} = 360$Å. 360Å is approximately the thickness of three steps of the pyramid or growth spiral of polyethylene.[10] One concludes, then, that if the illumination is strictly monochromatic with $\lambda = 5461$Å (mercury emission line), and if the per cent of light reflected is 90 or better at each surface, then the bright fringes extend over three steps of the growth spiral.

The bright fringes contour regions of constant optical path in the crystal illuminated. When the fringes are very narrow in width, small changes in optical path can be observed as displacements in the bright fringes. The narrower the fringe observed, the better small changes in fringe displacement (changes in optical path) can be detected, i.e., the better is the resolution in depth.

When growth spirals are illuminated normally, the fringe width is limited by the area of the steps exposed

where the constructive interference is occuring. In this case, the fringes need not necessarily be narrow, as for example would occur if a crystal were of thickness $\frac{\lambda}{2\mu}$:

Polyethylene crystals are biaxial, as will be discussed, and so possess three principal indices of refraction. If the light is propagated along one of the principal index directions, then only the other two indices need be considered in the equation which gives the thicknesses at which constructuve interference occurs, $t = \frac{n\lambda}{2\mu}$. There will then be two bright rings or rhomboids, one wherever:

$$t_1 = \frac{n\lambda}{2\mu_1} ,$$

and one wherever:

$$t_2 = \frac{n\lambda}{2\mu_2}$$

As it turns out, these two refractive indices of polyethylene ($\alpha = 1.515$, $\beta = 1.520$) are so close that the lines were not found separated (Figs. 16--19).

Figure 16 is a photomicrograph of a polyethylene growth spiral illuminated with parallel monochromatic light incident normally onto its bottom surface ($\lambda = 5461$Å). The crystal specimen was deposited onto a silvered optical flat and the system resilvered (as described in the experimental details following). Two bright rhombic lines are clearly visible, outlining the (110) faces of the crystal.

Each represents a thickness of $\frac{n\lambda}{2\mu}$, where μ is taken as the average of α and β (μ_1 and μ_2), i.e., $\mu = \frac{\mu_1 + \mu_2}{2} =$ 1.517. Substituting the values of μ and λ in the equation for t above, one has:

$$t = \frac{2(5461\text{Å})}{2(1.517)} = 3600\text{Å}$$

for the thickness up to the second (inner) line. The thickness of the crystal is obviously greater, for otherwise the inner bright line would be a region of brightness, and not have a dark interior. The thickness of this crystal could be anywhere from slightly greater than 3600Å to slightly less than $3600\text{Å} + \frac{\lambda}{2\mu} = 5400\text{Å}$, or one could write the thickness t as:

$$t = 4500 \pm 900\text{Å}.$$

The crystals of Figs.17--19 show more lines than does the crystal of Fig. 16 . The thickness of each of these crystals is less certain than that of Fig. 16 , since the lines in the interior of the last inner distinct fringe are muddled. This is caused either by improper focusing on the top of the pyramid (with the bottom of the pyramid in focus) or by the mixing of the fringes due to the sharp increase in thickness as one ascends the pyramid.

Figure 20 is a photomicrograph of a polyethylene growth spiral illuminated under similar conditions as above, but with the light from an unfiltered mercury lamp. One sees

that the inner lines are twisted with respect to the outer lines. This may occur due to the way the crystal settles onto the slide before being resilvered, or could be a crystal of the type shown in Fig. 12 . The crystal of Fig. 12 would clearly show a twisted inner fringe system when silvered as above. The illumination with polychromatic light merely facilitated this observation.

Figure 21 is a polyethylene growth spiral illuminated in the same way as the crystal of Fig. 20 . The crystal happened to be comparatively large and so makes some qualitative observations easier. The crystal must be a symmetrical pyramid, similar to Fig. 40 , and not as Fig. 12 . Parts of the crystal have not settled onto the slide as have adjacent regions, as the dark regions protruding into the bright regions show. Perhaps these darker regions are places where the crystal has not slipped or incompletely slipped, as Fig. 10 shows schematically. At any rate, each fringe is a region of constant optical path, and, if the surfaces of the crystal are flat, also of constant thickness.

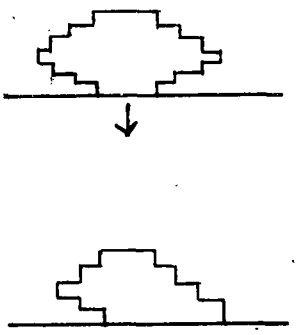

Figure 10

An extension of this method of multiple beam interferometry is to use silvered surfaces which are inclined to each other. This technique

gives fringes which are extremely thin with respect to width, allowing the resolution of distances as small as three Angstrom units in depth, as Tolansky has discussed.[8]

Finally the method used by Courtney-Pratt for the determination of thicknesses of the order of 20Å will be discussed.[9] This investigator deposited crystals of stearic acid onto a thin mica crystal. The surfaces of this system were then silvered. Illumination of the region near the stearic acid crystal with parallel monochromatic light allows the determination of n, the order of the interference fringe pattern, if the thickness of the mica crystal is known. Next, the crystal system was illuminated with parallel white light at normal incidence on the mica crystal. The mica crystal will transmit only certain wavelengths governed by the relation:

$$\lambda = \frac{2\mu t}{n} . \tag{15}$$

The region where the stearic acid crystal is located allows a slightly different wavelength to be transmitted, the wavelength difference being:

$$\Delta\lambda = \frac{2\mu}{n} (\Delta t \quad , \tag{16}$$

where Δt is the small change in thickness = thickness of the stearic acid crystal.

The light transmitted by the crystal was focused onto the slit of a spectroscope, where the wavelengths were measured. The stearic acid crystal was found to be 19 ± 3Å in thickness.

c) Experimental

The deposition of the silver onto the surfaces was effected through evaporation of the metal under high vacuum. The polyethylene crystals were deposited from their crystallization liquid (4.94 mg. polymer/g. toluene; crystallized at 90°C. with slow cooling) onto a silvered optical flat or microscope slide. This system was then resilvered, so that there was a layer of silver at the top and bottom surfaces of the crystal.

The quantity of silver deposited onto each surface of the crystal determines the amount of light reflected and so determines r. This amount could be followed during the course of the evporation by means of an oscillating quartz crystal. This quartz crystal was mounted next to the polyethylene crystals, so that both received the same amount of silver per $cm.^2$ As the silver was deposited onto the quartz crystal its mass changed and so its frequency of oscillation also changed. The change in frequency as a function of the percent of light reflected by the silver film was known and so r was determined at any time during the evaporation.[21a]

Tolansky has discussed the thickness of the evaporated silver films as a function of r and found that films of approximately 500Å - 700Å were best, with r = 0.95[6].

Using the density of silver, and knowing the weight of deposited silver and the area of the slide exposed, one could determine the film thickness. This would give a check on the quartz crystal.

The optical flat was weighed before and after a silver film was evaporated onto it. The weight of deposited silver was found to be 0.0047 g. The area of the flat exposed was 44.1 cm.^{2}. This gives 0.000107 g./cm.^{2} for the weight of silver/cm.^{2} of flat. With the density of silver 10.5 g./cm.^{3}, one finds that the thickness of the silver film in this instance is (approximately) 1000Å. The change in frequency of the quartz oscillator was 1200 cps., for which r was quoted as 0.95. Since films of approximately 600Å have an r value of 0.95 according to Tolansky, the film of 1000Å must have r at least 0.95.

The distance from the silver source to the crystal specimen was typically 11 cm. The source was about 5 cm. in extent, so that the length of the optical flat or microscope slide was paralleled with the source. The thickness of the silver film over the area of a polyethylene crystal should be approximately constant, since the crystals are only about 10^{-2} mm^2. in area.

An ordinary mercury lamp was found suitable for the observation of these crystals when the light was unfiltered.

Use of a filter for the 5461Å line of the mercury spectrum reduced the intensity severely, and the use of a high pressure mercury lamp was found necessary. The light was rendered parallel by focusing the lamp image onto a pin-hole, which was located at the focal point of a lens. The light emerging from the lens was then parallel and was arranged so as to be incident normally onto the crystals (see diagram below, Fig. 11).

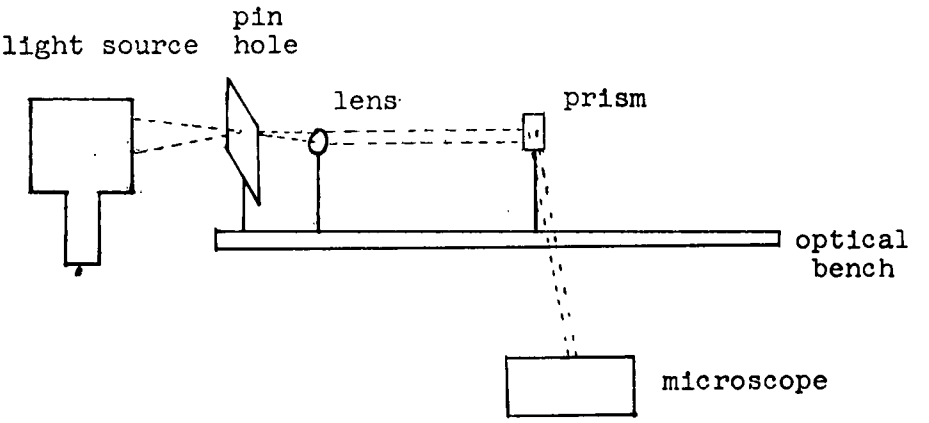

Figure 11

1. (a) Till, J. Polymer Sci., 24, 301 (1957); (b) Fischer, Z. Naturforsch., 12a, 753 (1957); (c) Keller, Phil. Mag., 2, 1171 (1957).

2. Geil, Symons and Scott, J. Appl. Physics, 30, 1516 (1959).

3. Geil, J. Polymer Sci., 44, 449 (1960).

4. Keller and O'Connor, Disc. Faraday Soc., 25, 114 (1958).

5. Anderson and Dawson, Proc. Roy. Soc., 218, 255 (1953).

6. Tolansky, Surface Microtopography, Interscience Publ., Inc., N.Y., N.Y. (1960).

7. Francon, Prog. in Microscopy, vol. 9, Row, Peterson and Co., N.Y., N.Y. (1960).

8. Dawson and Vand, Proc. Roy. Soc., 206, 555 (1951).

9. Courtney-Pratt, Proc. Roy. Soc., 212, 505 (1952).

10. Wunderlich and Sullivan, J. Polymer Sci., 56, 19 (1962).

11. Geil and Statton, J. Appl. Polymer Sci., 3, 357 (1960).

12. American Optical Co., Buffalo 15, N.Y.

13. Nomarski and Weill, Bull. Societe francaise mineralogie, 77, 840 (1954).

14. Born and Wolf, Principles of Optics, Pergamon Press, N.Y., N.Y. (1959).

15. Khoury and Padden, J. Polymer Sci., 47, 455 (1960).

16. Keller, Polymer, 3, 393 (1962).

17. Jenkins and White, Fundamentals of Optics, McGraw-Hill Book Co., N.Y., N.Y. (1957).

18. Wunderlich and Sullivan, J. Polymer Sci., 61, 195 (1962).

19. Kamb, Amer. Miner., 43, 1029 (1958).

20. Forty, Phil. Mag., 43, 377 (1952).

21. Verma and Reynolds, Proc. Phys. Soc., 66B, 414 (1953).
(a) the use of the apparatus of Mr. D. Berkeley is gratefully acknowledged.

SUMMARY

Single crystals and dendrites of polyethylene have been grown from dilute solution. The degree of supercooling at the time of crystallization determines the mode of growth.

For the measurement of single crystal platelet and growth spiral thicknesses, the Baker interference microscope was used. In the most favorable case, the precision was $\pm$6Å for the thickness of a platelet.

The Nomarski interferometer was used on a polarizing incident light microscope. This system was employed for the observation of platelets and growth spirals, as well as for the determination of melting points of the latter.

Growth spirals and single crystals show insufficient contrast for observation with an ordinary optical microscope. If one silvers the top and bottom surfaces of the crystals, the multiple beam interference patterns allow the observation of the platelets and growth spirals. In this way any optical microscope can be used for polymer crystals work.

The use of Newton's rings method of interferometry is also discussed for the measurement of polymer crystal thicknesses.

Upper left, Figure (12), A growth spiral of polyethylene photographed with the Namarski attachment on a Reichert incident light microscope. Sample grown from tetrachloroethylene at 80.7°C. The magnification is 500x.

Upper right, Figure (13), Single crystals of polyethylene photographed with the Baker interference microscope. Same sample as in Fig. 12. 620x.

Lower left, Figure (14), Single crystals and growth spirals of polyethylene photographed as in Fig. 13. The sample and magnification are the same.

Lower right, Figure (15), A polyethylene twinned crystal with growth spirals photographed as in Fig. 13. The sample and magnification are the same.

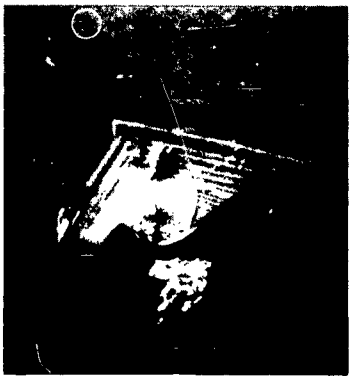

Fig.

Fig.

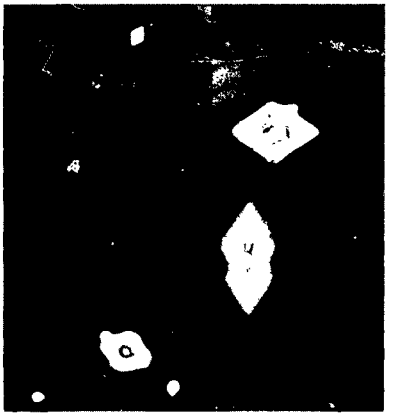

Fig.

Fig.

Upper row, Figures (16-19), Polyethylene growth spirals, the top and bottom surfaces of which have been silvered. The illumination is monochromatic (λ = 5461Å). The sample was grown from toluene at 90.3°C. These crystals are viewed in transmitted light with an ordinary microscope at a magnification of 490x.

Second row, Figures (20-21), Polyethylene growth spirals viewed as in Figs. 16--19, but with unfiltered mercury illumination. The sample was grown from toluene at 90.8°C.

Third row left, Figure (22), The Newton's rings interference system. The radius of the contact lens is 3.0 mm.

Third row right, Figure (23), The normal paraffin $C_{36}H_{74}$ photographed with the Nomarski attachment on the Reichert incident light microscope. The magnification is 130x.

Bottom right, Figure (24), Same sample as in Fig. 23 photographed with the lens of Fig. 22 in contact with the surface of the microscope slide.

Bottom left, Figure (25), Same interference system in Fig. 22, except that the microscope slide and contact lens have been silvered.

Fig.

Fig.

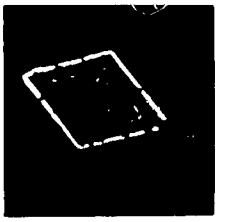

Fig.

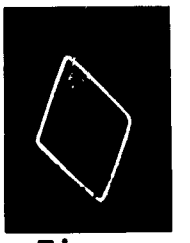

Fig.

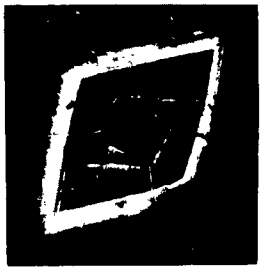

Fig.

Fig.

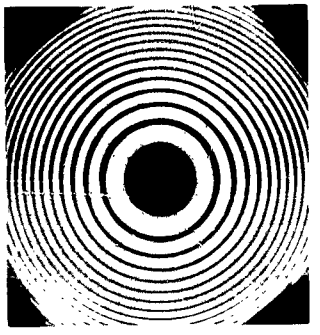

Fig.

Fig.

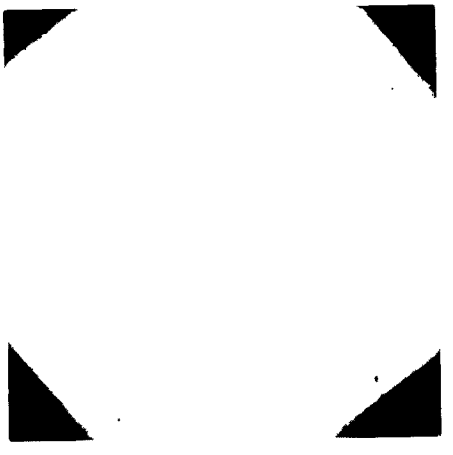

Fig.

Fig.

Upper left, Fig. (26), Polyethylene needles photographed with the Baker interference microscope. The sample was grown from chlorobenzene-toluene (see text) at 89.7°C. The magnification is 620x.

Upper right, Fig. (27), A polyethylene dendrite photographed as in Fig. 26. The sample was grown from toluene.

Center left, Fig. (28), Polyethylene growth spirals photographed as in Fig. 12. The sample was grown from toluene at 89.1°C. Fig. 28a was taken at room temperature and Fig. 28b after melting. The magnification is 185x.

Center right, Fig. (29), Same sample as in Fig. 28, but different crystals. Photographed as in Fig. 28. The larger growth spiral melted at 126.8°C. under a heating rate of 3°C/min. at melting.

Bottom left, Fig. (30), A polyethylene growth spiral photographed as in Figs. 20--21. The sample is from toluene at 90.3°C.

Bottom center, Fig. (31), Same crystal as in Fig. 30, but photographed with monochromatic light (λ = 5461Å).

Bottom right, Fig. (32), Same crystal as in Fig. 30 photographed as in Fig. 12. Magnification is 500x.

Fig.

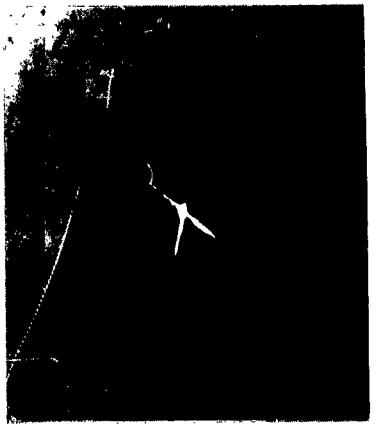

Fig.

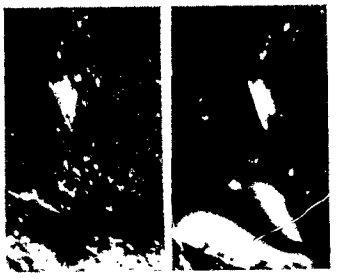

(a) (b)

Fig.

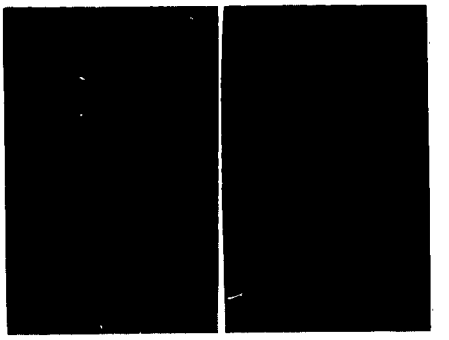

(a) (b)

Fig.

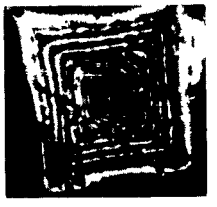

Fig.

Fig.

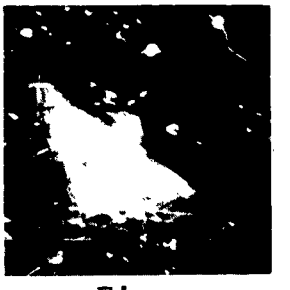

Fig.

Fig. 33. The ratio of the transmitted light I_t to the incident light I_o as a function of the crystal thickness t. The angle of incidence of the light is zero, i.e., the light is incident normally onto the crystal surface. The case r = 0.2 for polyethylene crystals. The case of r = 0.9 is for silvered polyethylene crystals.

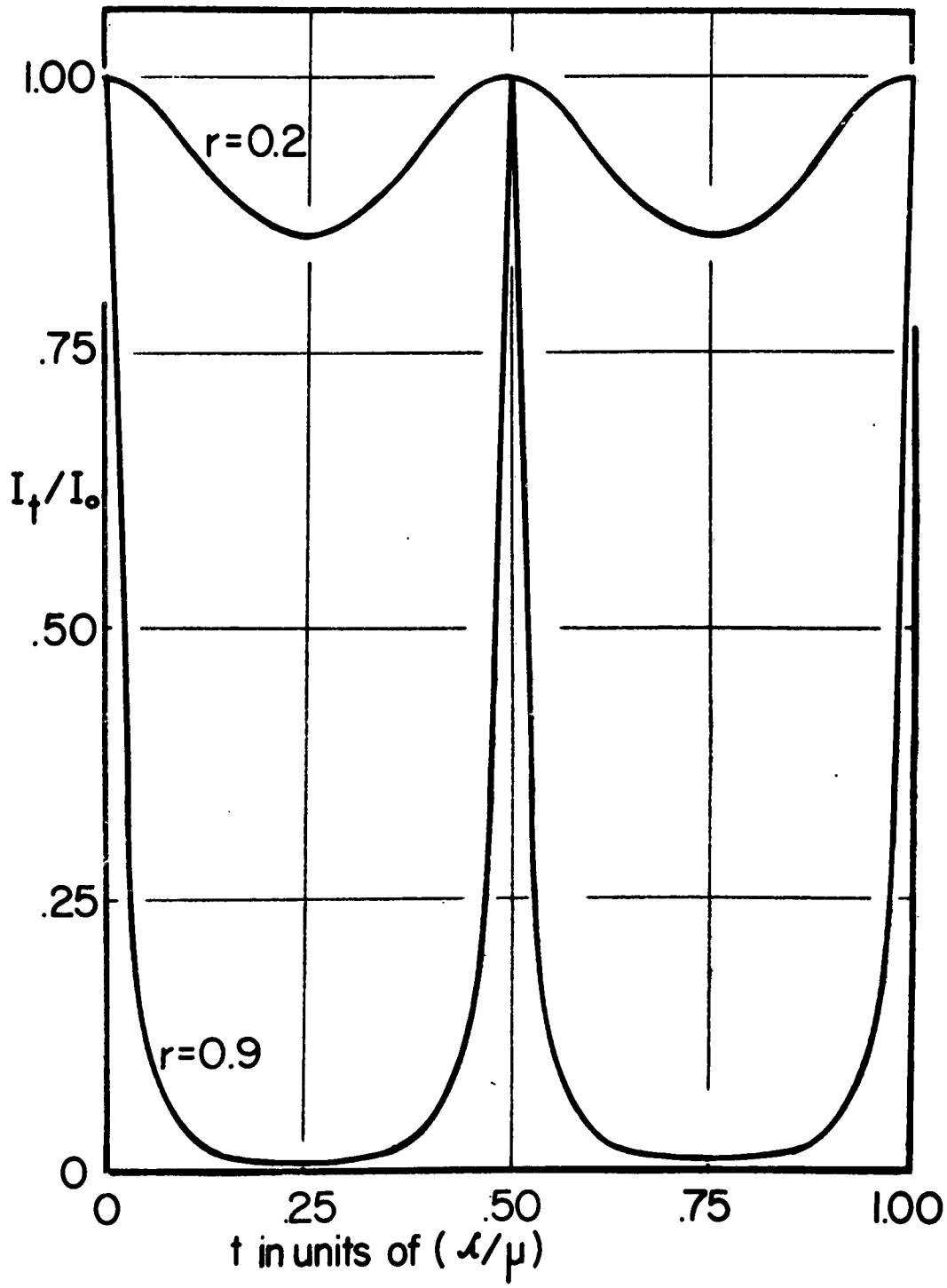
1.00
.75
.50
.25
0
I_t/I_o
r=0.2
r=0.9
0
.25
.50
.75
1.00
t in units of (λ/μ)